VOL. 7, NO. 9, SEPTEMBER 2012 ISSN 1819-6608
ARPN Journal of Engineering and Applied Sciences


www.arpnjournals.com

# AERODYNAMIC DRAG REDUCTION IN A PASSENGER VEHICLE USING VORTEX GENERATOR WITH VARYING YAW ANGLES

Gopal P.[1] and Senthilkumar T.[1]
[1]Department of Automobile Engineering, Anna University of Technology, Tiruchirappalli, Tamil Nadu, India
E-Mail: rameshkumaratvellore@gmail.com, gopalpp@gmail.com

**ABSTRACT**

Large investments are aimed at minimizing power needed for propulsion i.e., new downsized engines with new aerodynamic devices for drag reduction. For passenger vehicles the aerodynamic drag force is the dominating resistance force at higher velocity. The vehicle body is often optimized for reducing the drag resistance. Vortex generators belong to the category boundary layer manipulators. Their function is to reenergize an adverse pressure gradient boundary layer that is about to separate by transporting high momentum fluid from the outer part of the boundary layer down to the low momentum zone closer to the wall. In this experimental investigation the variation of pressure coefficient, dynamic pressure, coefficient of lift and drag with and without vortex generators (VG) on the roof of a utility vehicle have been studied at varying yaw angles of VG. The yaw angles used are 10˚, 15˚ and 20˚. To measure the effect of altering the vehicle body, wind tunnel tests have been performed with 1:15 scaled model of the utility vehicle with velocities of 2.42, 3.7, 5.42 and 7.14m/s. The experiments showed that a great improvement of the aerodynamic drag force reduction can be achieved with vortex generator.

**Keywords:** passenger vehicle, aerodynamics, vortex generator, pressure coefficient, dynamic pressure, boundary layer, wind tunnel, yaw angle.

## 1. INTRODUCTION

A vortex generator is an aerodynamic surface which is basically a small vane that creates a vortex. They can be found in many systems like aircraft, ships, turbines, ground vehicles etc. Vortex generators are added to maintain steady airflow over the control surfaces at the rear of the wing. They are typically rectangular or triangular in shape of about 1 or 2 cm in size [1]. There have been recent developments in using vortex generators for passive control of shock/boundary-layer interactions, involving both experiment and computations. The precise mechanisms of how they function at high speeds remain the subject of debate [2-4, 5-8]. Studies indicate that vortex generators modify the inner structure of the boundary layer to make the layer more resistant to separation. Some investigators suggest that the trailing vortices provide the mixing with the free stream to energize the boundary layer. However, apparently no experimental or computational results have been obtained to support this suggestion. A practical advantage of vortex generators is their small size which results in less drag than their conventional counterparts [9-12]. The primary objective of this study is to investigate the aerodynamic effects of adding vortex generator (VG) and their impact on fuel consumption. A motor vehicle travelling at a constant velocity on a level road, the power required to overcome the aerodynamic drag (approximately 80%) and tyre rolling resistance (around 20%). However, with an increase of speeds, the required power increases significantly to overcome aerodynamic resistance (drag) while power required for rolling resistance remain almost constant as given in Equation (1).

$$\text{Power}_{(\text{Required})} = C_D \tfrac{1}{2} \rho A V^3 \quad (1)$$

Although the primary focuses of vehicle manufacturers and researchers have been concentrated on fuel saving devices of the commercial vehicles till to date. As the number of passenger cars have been increased significantly worldwide, it becomes important to study the aerodynamic effects of utility vehicle. Hence in this work, the variation of pressure coefficient and dynamic pressure with and without vortex generators (VG) on the roof of a utility vehicle have been investigated at varying yaw angles of VG.

## 2. EXPERIMENTAL DETAILS

### 2.1 Design of VG

In order to find a viable configuration, one must first identify the important variables for vortex generator design. In order to reduce the degrees of freedom, most of the variables were fixed based on either analysis or recommendations of previous researchers [13]. A Single vane type delta (triangular) shaped was chosen. Due to their simplicity and widespread usage, the low drag device than any other type makes the vane type more suitable for attaching on the vehicle body. Delta shaped VG's were most commonly used on aircraft wings [14]. In connection with the height, the thickness of the boundary layer is measured based on the assumption that the optimum height of the VG would be nearly equal to the boundary layer thickness. Figuire-1 shows the velocity profile on the vehicle's roof. From Figure-1, the boundary layer thickness at the roof end immediately in front of the separation point is found to be about 2 mm. Consequently, the optimum height for the VG is estimated to be up to approximately 2 mm. The thickness of VG was fixed at 0.5 mm uniform throughout so as to make a stiffened structure.

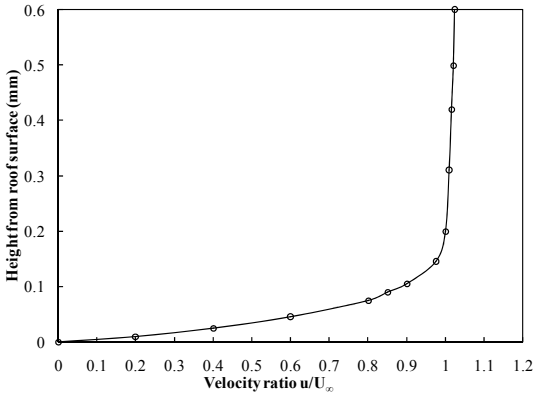


**Figure-1.** Velocity profile on roof.

Length was taken in proportion of the height of the VG. In these experimental work L/H ratio was taken as 2 with the Interval to height ratio of 6. Based on this ratio, a single row of VG was positioned on the roof with 8 numbers of VG as shown in Figure-2 and the arrangement of VG is shown in Figure-3.

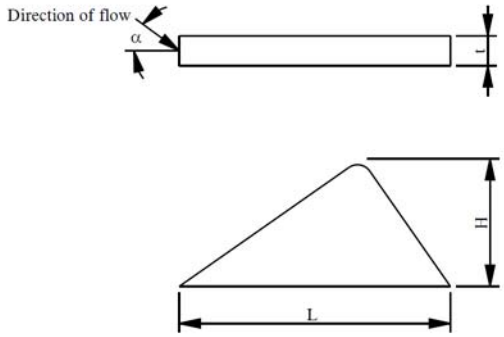


**Figure-2.** Dimensions of VG.

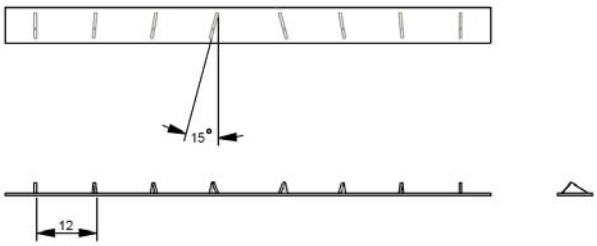


**Figure-3.** Arrangement of VG in a row.

This parameter describes the spacing between VG in a row. One row of VG was fixed at 5 mm from the roof end. This point was fixed, based on the boundary layer measurements and separation point of the stream line on the roof. The number of row was limited to one in order to minimize weight and potential manufacturing cost. The delta shaped VGs is installed at varying yaw angle of 10°, 15° and 20° to the airflow direction. But the airflow direction was found to be different between sideways positions on the roof. The airflow is aligned directly with the backward direction at center of a vehicle, but it increasingly deviates toward the center as the measurement point shifts away from the central position.

### 2.2 Scale model and experimental setup

The test model used was Tata Sumo Grande with a scale ratio of 1:15. The scale model of the vehicle is shown in Figure-4. The length, breadth and height of the scaled model are was 0.295 m, 0.108m and 0.1m respectively. Thickness of the sheet metal used was 0.5mm. The Vortex generators were cut into pieces from the sheet metal and they were fixed on to a base plate by gas welding process. The base plate with VG was fastened to the roof of scaled model by means of bolt and nut. To measure the static pressure on the body, 0.2 mm diameter holes were drilled on the centre line of the vehicle body starting from the front end along the roof to the rear end of the vehicle as shown in Figure-5. 15 pressure tappings are used. Out of which five of them are on the roof, three on the rear end and remaining seven are on the front end of the vehicle. Pressure tubes are fixed from inside of the holes. Pressure tappings are connected to micro manometer using pressure tubes.

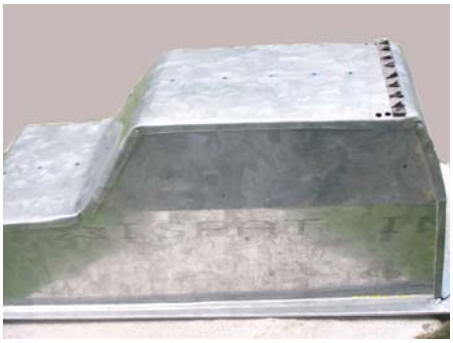

**Figure-4.** Scale model

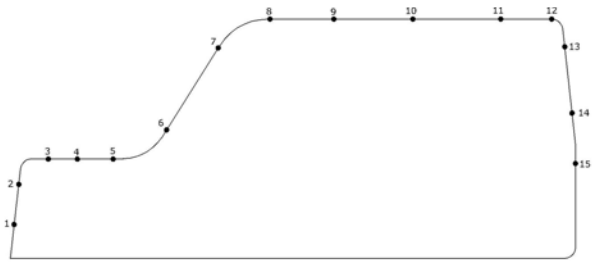


**Figure-5.** Location of manometers.

An open circuit wind tunnel (Altech, India) with a test section of 0.09 $m^2$ was used. The schematic of the wind tunnel is shown in Figure-5. The total length of the wind tunnel was 6m and the test section length was 1 m. A 25 HP electric motor was used for suction. The pressure data were not corrected for horizontal buoyancy as the static pressure gradient in the wind tunnel was deemed negligible. The wind tunnel tests were conducted at positive and negative yaw angles between ±15°. The

frontal area of the scale model of the vehicle is 0.0108 $m^2$. The blockage ratio is calculated to be about 9.2%. The relative air speed was measured by using micro manometer (Furnace control ltd, UK) in wind tunnel test section. This relative air speed was measured to calculate the dynamic pressure variations along the centre line of vehicle body. A micro manometer has an accuracy of ± 0.5 %. Velocity uniformity is ±0.96% which is 1% as given in SAE Wind Tunnel Test procedure [15].

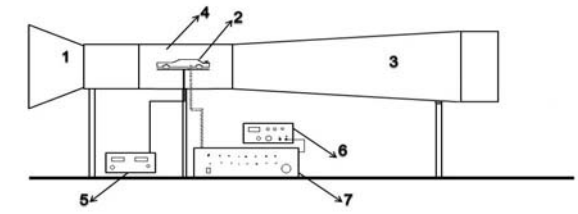


1-Air Filter
2-Car Model
3-Axial Fan Duct
4-Test Section
5-Force Display Unit
6-MicroManometer
7-20 Line Single Way Selection Box

**Figure-5(a).** Experimental setup.

### 2.3 Experimental procedure

The experiment was done with an objective of measurement of drag force, pressure variations and relative speed with varying speeds along the centre line of the vehicle under straight wind conditions. The pressure points are observed on the front, the roof and the rear. The pressure tubes are connected from the model to 20-Way single Selection box and then to the Digital Manometer and the pressure difference is observed. For calculating Drag and lift force load cell directly attached to platform on which vehicle model is fixed was used as transducer which changes the variation of position due to force in equivalent change in resistance, that change in resistance is converted in numerals by means of display unit as shown in Figure-6.

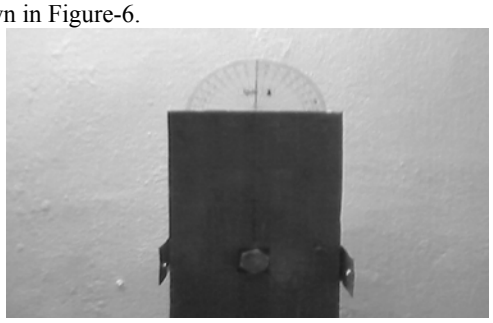

**Figure-6.** Platform on which model is fixed.

## 3. DATA REDUCTION

### 3.1 Pressure coefficient

The pressure coefficient is a dimensionless number which describes the relative pressures throughout a flow field in fluid dynamics. The pressure coefficient is a very useful parameter for studying the flow of incompressible fluids such as water, and also the low-speed flow of compressible fluids such as air. The relationship between the dimensionless coefficient and the dimensional numbers is given in Equation (2).

$$C_p = \left(p - p_\infty\right)/\left(\rho_\infty V_\infty{}^2\right) \quad (2)$$

### 3.2 Dynamic pressure

Bernoulli's equation for incompressible flow is given by the Equation (3).

$$P_\infty = p + \left(\rho/2\right) * u^2 = const \quad (3)$$

The above equation relates pressure and velocity along a stream line. According to Bernoulli's equation total pressure is the sum of static pressure and dynamic pressure. The equation indicates low pressure in regions of high local velocities and vice versa.

### 3.3 Coefficient of drag

The drag force is the component of the resultant force parallel and opposite to the flow. The drag coefficient ($C_D$) is obtained experimentally through the vehicle geometry or form, and it allows the results do not depend on the real dimensions of the vehicle. The $C_D$ represents the relation between drag force and the force of the relative fluid, being expressed by the Equation (4).

$$D = \frac{1}{2} C_D \rho A V^2 \quad (4)$$

### 3.4 Coefficient of lift

The lift force is the component of the resultant force perpendicular and opposite to the flow. The lift coefficient ($C_L$) is obtained experimentally through the vehicle geometry or form, and it allows the results do not depend on the real dimensions of the vehicle. The $C_L$ represents the relation between lift force and the force of the relative fluid, being expressed by the Equation (5).

$$L = \frac{1}{2} C_L \rho A V^2 \quad (5)$$

## 4. RESULTS AND DISCUSSIONS

### 4.1 Pressure coefficient

Figure-7 shows the variation of pressure coefficient along the X coordinates of the scale model at a free stream velocity of 2.42 m/s. From the figure it is observed that the value of pressure coefficient without VG is minimum at the x coordinate of about 240 mm, whereas its value is maximum with VG having a yaw angle of 15°. It is due to the fact that the thickness of the boundary layer is nearly equal to the height of VG at a yaw angle of 15°. Figures 8, 9 and 10 shows the variation of pressure coefficient along the X coordinates of the scale model at a

free stream velocity of 3.7, 5.42 and 7.14 m/s, respectively. It is evident that the values of pressure coefficient don't change significantly with increase in velocity for various values of yaw angle. This can be attributed to the fact that the boundary layer thickness is inversely proportional to Reynolds number and hence at higher velocities i.e., at higher Reynolds number the boundary layer thickness becomes too small and hence the effect of varying yaw angle of VG could not be realized. However, it is interesting to observe that the pressure coefficient can be increased with the inclusion of VG by around 17% at a velocity of 7.14 m/s. Similarly the pressure coefficient can be increased with the inclusion of VG to a maximum of around 19% and 10 % at a velocity of 5.42 and 3.7 m/s respectively for a yaw angle of 15˚.

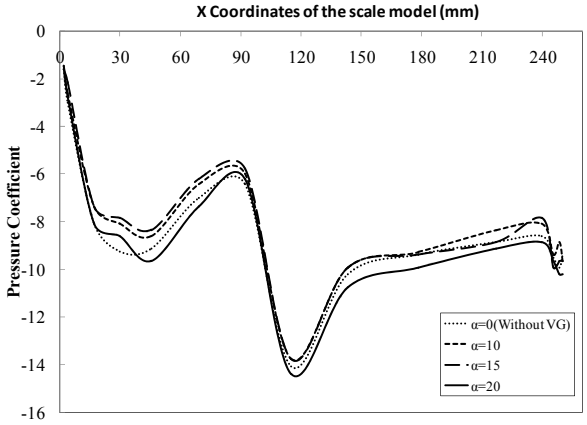


**Figure-7.** Variation of $C_p$ at $U_\infty$ = 2.42 m/s for different values of yaw angle.

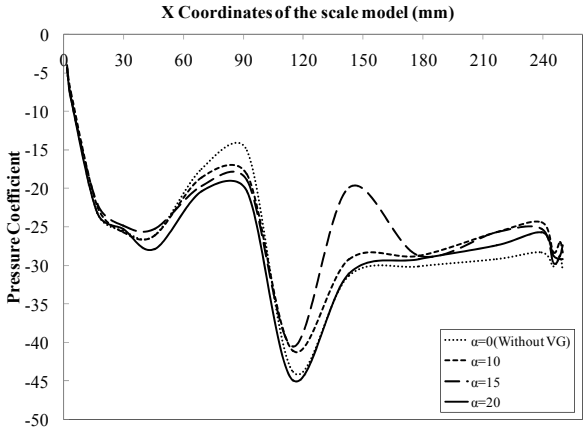


**Figure-8.** Variation of $C_p$ at $U_\infty$ = 3.7 m/s for different values of yaw angle.

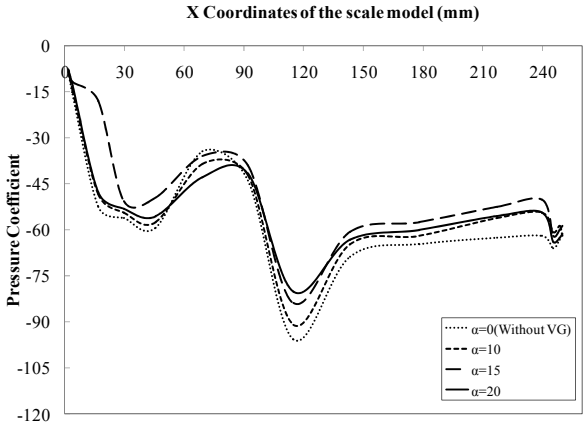


**Figure-9.** Variation of $C_p$ at $U_\infty$ = 5.42 m/s for different values of yaw angle.

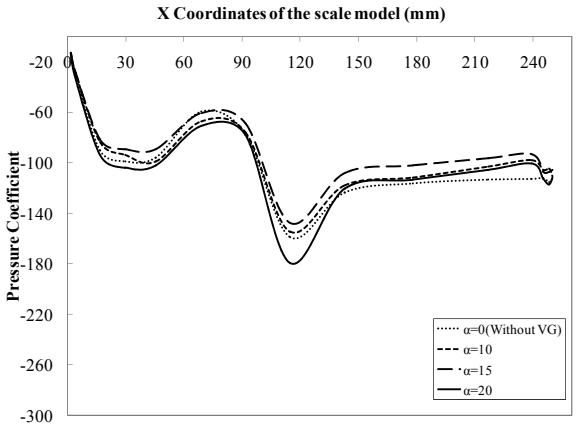


**Figure-10.** Variation of $C_p$ at $U_\infty$ = 7.14 m/s for different values of yaw angle.

### 4.2 Dynamic pressure

Figure-11 shows the variation of Dynamic pressure along the X coordinates of the scale model at a free stream velocity of 2.42 m/s. From the figure it is observed that the value of dynamic pressure without VG is maximum at the x coordinate of about 240 mm, whereas its value is minimum with VG having yaw angle of 15°. The results shows that the dynamic pressure over the surface of the vehicle roof increases with addition of VG which is favorable for avoiding flow separation and the consequent losses. Figures 12, 13 and 14 shows the variation of dynamic pressure along the X coordinates of the scale model at a free stream velocity of 3.7, 5.42 and 7.14 m/s respectively. It is evident that the values of dynamic pressure don't change significantly with increase in velocity for various values of yaw angles. However, it is interesting to observe that the dynamic pressure can be increased with the inclusion of VG by around 19% at a velocity of 7.14 m/s. Similarly the dynamic pressure can be increased with the inclusion of VG to a maximum of around 24% and 18 % at a velocity of 5.42 and 3.7 m/s respectively for yaw angle of 15°.

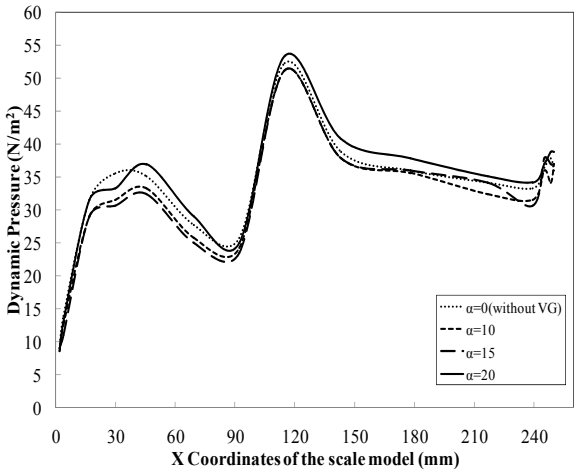


**Figure-11.** Variation of $P_d$ at $U_\infty$ = 2.42 m/s for different values of yaw angle.

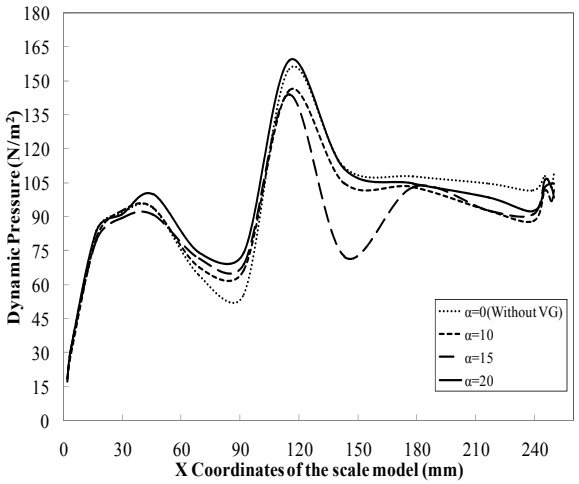


**Figure-12.** Variation of $P_d$ at $U_\infty$ = 3.7 m/s for different values of yaw angle.

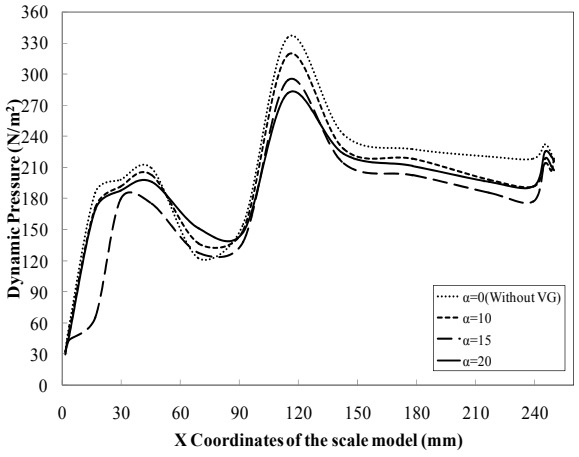


**Figure-13.** Variation of $P_d$ at $U_\infty$ = 5.42 m/s for different values of yaw angle.

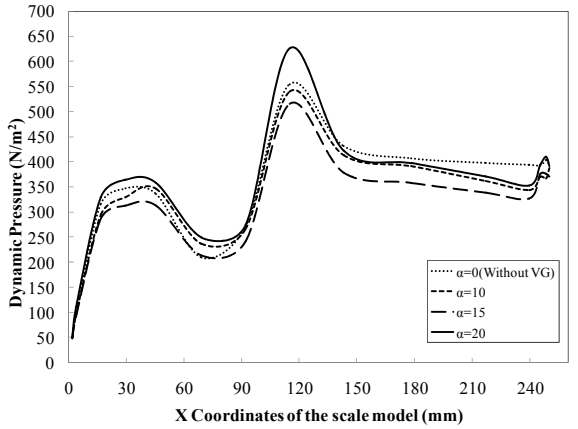


**Figure-14.** Variation of $P_d$ at $U_\infty$ = 7.14 m/s for different values of yaw angle.

### 4.3 Coefficient of drag

Figure-13 shows the variation of $C_D$ values for different values of yaw angles at varying free stream velocities along the longitudinal centre plane of the scale model. It is clearly evident from the figure that the value of $C_D$ decreases due to the addition of VG. This can be attributed due to the avoidance of flow separation with the help of VG. For instance at a velocity of 2.42 m/s the coefficient of drag is reduced by a maximum of 90% when VG with a yaw angle of 15˚ is used when compared to the values obtained without VG. Similarly at same velocity a minimum of 20% reduction in drag is obtained for VG with a yaw angle of 10˚. For varying value of yaw angle, the $C_D$ remains constant for increase in velocity. However when angle yaw is increased the $C_D$ values varies with increase in velocity. Hence, it is observed that VG with a yaw angle of 15˚ will be useful at lower velocity.

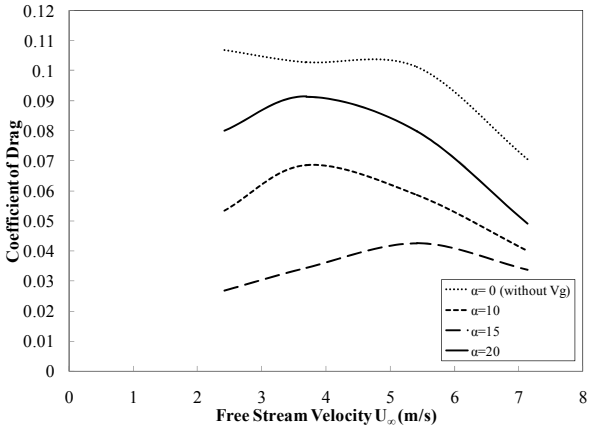


**Figure-15.** Variation of $C_D$ for different values of yaw angle along the centre plane.

### 4.4 Coefficient of lift

Figure-14 shows the variation of $C_L$ values for different values of yaw angles at varying free stream velocities along the longitudinal centre plane of the scale

model. It is clearly evident from the figure that the value of $C_L$ decreases due to the addition of VG. This can be attributed due to the avoidance of flow separation with the help of VG. For instance at a velocity of 2.42 m/s the coefficient of lift is reduced by a maximum of 85% when VG with a yaw angle of 15˚ is used when compared to the values obtained without VG. Similarly at same velocity a minimum of 50% reduction in lift is obtained for VG with a yaw angle of 10˚. However the value of $C_L$ decreases with increase in velocity with and without VG. The results revealed that at higher velocity the value of $C_L$ remains constant for VG of all yaw angles.

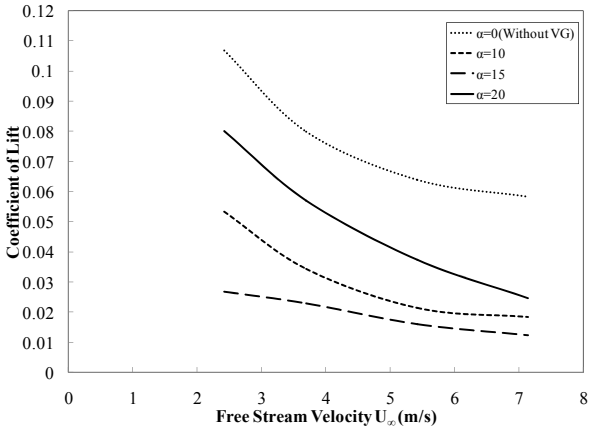


**Figure-16.** Variation of $C_L$ for different values of yaw angle along the centre plane.

## 5. CONCLUSIONS

From the experimental investigation on the measurement of the variation of pressure coefficient and dynamic pressure on the roof of a utility vehicle with and without vortex generators (VG), the following conclusions were made:

a) The value of pressure coefficient without VG is minimum whereas its value was observed to be maximum with VG having yaw angle of 15°.
b) The pressure coefficient can be increased with the inclusion of VG by around 17% at a velocity of 2.42 m/s.
c) The values of pressure coefficient don't change significantly with increase in velocity for various values of yaw angle.
d) Dynamic pressure over the surface of the vehicle roof increases with addition of VG which is favourable for avoiding flow separation and the consequent losses.
e) The value of $C_D$ is reduced by 90% with the addition of VG at a velocity of 2.42 m/s and a minimum of 20% reduction in drag is obtained for VG with a yaw angle of 10˚
f) It is observed that VG with a yaw angle of 15˚ will be useful at lower velocity
g) The value of $C_L$ decreases with increase in velocity with and without VG and the results revealed that at higher velocity the value of $C_L$ remains constant for VG with varying yaw angles.

## Nomenclature

| Symbol | Meaning | Unit |
|---|---|---|
| D | Drag force | N |
| L | Lift force | N |
| CD | Drag coefficient | - |
| CL | Lift coefficient | - |
| Re | Reynolds number | - |
| U∞ | Velocity of air | m/s |
| ρ | Density of air | $kg/m^3$ |
| A | Projected area | $m^2$ |
| S | Distance Travelled by vehicle | m |
| Cp | Pressure coefficient | - |
| u | Relative speed of air | m/s |
| P | Static pressure | $N/m^2$ |
| P∞ | Total pressure | $N/m^2$ |
| L | Fuel consumption | Lit/Hr |
| $P_d$ | Dynamic pressure | $N/m^2$ |
| α | Yaw angle | degrees |

## REFERENCES

[1] C. H. K. Williamson. Three Dimensional Vortex Dynamics in Bluff Body Wakes.

[2] Alam F. and Watkins S. 2004. Aerodynamics of Trucks and Drag Reducing Devices. Journal of Mechanical Engineering, Khulna University of Engineering and Technology, Khulna, Bangladesh.

[3] Hucho W. H. 1998. Aerodynamics of Road Vehicles. 4th edition. Society of Automotive Engineers (SAE). ISBN 0-7680-0029-7, Warrendale, USA.

[4] Cooper K R. 2006. Full-Scale Wind Tunnel Tests of Production and Prototype, Second-Generation Aerodynamic Drag-Reducing Devices for Tractor-Trailers. SAE Paper No. 2006-01-3456, USA.

[5] Barlow J.B., Rae Jr., W. W. and Pope A. 1999. Low-Speed Wind Tunnel Testing, 3rd Edition. John Wiley and Sons, Inc. New York, NY, USA.

[6] RAS 66029. 1981. Subsonic Performance Data for NACA Type Submerged Air Intakes. Royal Aeronautical Society.

[7] Stephens A.V. 1957. Solid Boundary Surface for Contact with a Relatively Moving Fluid Medium. U.S. Patent No. 2, 800, 291. U.S. Department of Commerce, Washington DC, USA.

[8] Kuethe A.M. 1970. Boundary Layer Control of Flow Separation and Heat Exchange. US Patent. 3, 74 1,


285. U.S. Department of Commerce, Washington DC, USA.

[9] Landman D., Wood R. M and Seay W. S. 2009. Understanding Practical Heavy Truck Drag Reduction Limits. SAE Paper No. 2009-01-2890, USA.

[10] Schoon R. E. 2007. On-road Evaluation of Devices to Reduce Heavy Truck Aerodynamic Drag. SAE Paper 2007-01-4294, USA.

[11] Watkins S., Saunders J. W. and Hoffmann P. H. 1987. Wind Tunnel Modeling of Commercial Vehicle Drag Reducing Devices: Three Case Studies. SAE Paper No. 870717, Detroit, USA.

[12] Snyder R. H. 1977. Tire Rolling Losses and Fuel Economy. SAE Special Publication. Detroit, USA. p. 74.

[13] Image: http://www.carbodydesign.com/archive/2009/05/14-volkswagen-polo/VW-New-Polo-Wind-Tunnel-Testing-1-lg.jpg.

[14] Masaru koike, Tsunehisa Nagayoshi and Naoki Hamamoto. 2004. Mitsubishi Motors, Technical Review, No. 16.

[15] SAE Wind Tunnel Test Procedure for Trucks and Buses, Recommended Practice-July 1981- SAE J 1252.